

## Reduction of Viscosity in Suspension of Swimming Bacteria

Andrey Sokolov<sup>1,2</sup> and Igor S. Aranson<sup>2</sup>

<sup>1</sup>*Illinois Institute of Technology, 3101 South Dearborn Street, Chicago, Illinois 60616, USA*

<sup>2</sup>*Materials Science Division, Argonne National Laboratory, 9700 South Cass Avenue, Argonne, Illinois 60439, USA*

(Received 15 May 2009; published 29 September 2009)

Measurements of the shear viscosity in suspensions of swimming *Bacillus subtilis* in free-standing liquid films have revealed that the viscosity can decrease by up to a factor of 7 compared to the viscosity of the same liquid without bacteria or with nonmotile bacteria. The reduction in viscosity is observed in two complementary experiments: one studying the decay of a large vortex induced by a moving probe and another measuring the viscous torque on a rotating magnetic particle immersed in the film. The viscosity depends on the concentration and swimming speed of the bacteria.

DOI: 10.1103/PhysRevLett.103.148101

PACS numbers: 87.16.-b, 05.65.+b

The dynamics of self-propelled biological objects, such as bacteria, sperm cells, and locusts have attracted enormous attention in both the physics and biology communities [1–9]. Theoretical studies have predicted a plethora of dynamic instabilities, anomalous density fluctuations, and nontrivial stress-strain relations in such active nonequilibrium systems [10–12]. A phenomenological model of active particle suspensions [13] hinted that the viscosity becomes a function of the particles' activity. Recent analytical studies [14] indicate that the shear viscosity in a dilute suspension of swimmers can be smaller than the viscosity of the ambient liquid. Experiments with motile *E. coli* have shown that suspensions of bacteria may possibly violate the dissipation-fluctuation theorem and exhibit nonequilibrium rheology [15]. However, to date, there have been no direct experimental measurements of the shear viscosity of bacterial suspensions.

In this Letter we report on experimental studies of the viscosity of suspensions of *Bacillus subtilis*, a swimming aerobic bacterium, in freestanding liquid films. Depending on the concentration of bacteria and their activity (typical swimming speed), up to a sevenfold reduction in the viscosity was observed compared to that of the same suspension of nonmotile bacteria. The effect is interpreted as a transformation by the swimming bacteria of chemical energy from nutrients into mechanical energy of fluid motion, thus counterbalancing the energy loss due to viscous dissipation.

To measure the shear viscosity, we performed two complementary experiments in a wide range of bacterial concentrations and swimming speeds. In the first experiment, the viscosity was inferred from the decay time of a macroscopic vortex created in the film by a moving magnetically actuated probe. In the second experiment, the viscosity was extracted from measurements of the torque exerted on a rotating magnetic particle immersed in the film. The flow velocity was obtained from the trajectories of fluorescent tracers. The freestanding film configuration of our experimental cell allows control of the concentration of the

dissolved oxygen, and, thus, the swimming speed of the aerobic bacteria, which is difficult for standard rheology techniques.

Experiments were conducted on strain 1085 of *Bacillus subtilis*, a rod-shaped bacterium  $\sim 5 \mu\text{m}$  long and  $\sim 0.7 \mu\text{m}$  in diameter. The bacteria were grown in a TB medium (Sigma T5574), concentrated by centrifugation, and then placed in a fresh TB medium. In a typical experiment, the average concentration of bacteria in the TB medium was  $\sim 2 \times 10^{10} \text{ cm}^{-3}$ , which is approximately 20 times higher than in the stationary phase of growing. The computer-controlled experimental setups (see Figs. 1 and 4) were based on an earlier design [4] with a number of important modifications, discussed below. A  $10 \mu\text{l}$  drop of bacterial suspension was placed between two supporting crossed pairs of fibers, which formed a small square window. The drop was stretched to a thickness of  $\approx 200 \mu\text{m}$  by moving a supporting platform attached to one crossed pair of the fibers. The size of the square window in most of our experiments was  $7 \text{ mm} \times 7 \text{ mm}$ .

The speed of aerobic bacteria depends on the concentration of dissolved oxygen: lack of oxygen suppresses the motility of bacteria. To control the swimming speed, we replaced the air in the experimental chamber with nitrogen over a period of approximately 2 min. During this time, the

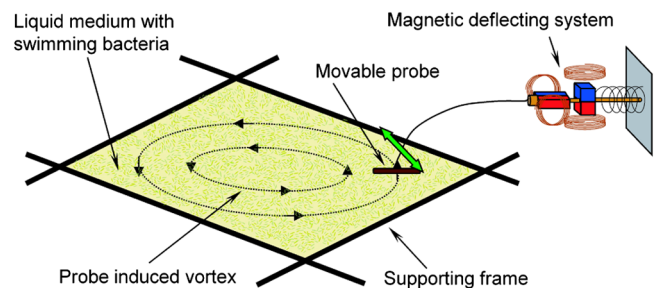


FIG. 1 (color online). Experimental setup 1: a thin liquid film with bacteria spans between four movable fibers. A micromanipulator with a magnetic deflecting system is used to initiate a large vortex through movement of the probe.

bacteria gradually reduced their swimming speed to zero (somewhat similar motility control of *E. coli* was used in [16]); see Fig. 2, inset. The swimming speed of bacteria was estimated using particle image velocimetry (PIV) (in relatively thin films), or from the trajectories of small fluorescent markers ( $0.53 \mu\text{m}$  in diameter, Red Nile, Spherotech) in thicker films where the direct tracking of bacteria becomes difficult. In thin films we observed that there is an almost linear relation between the speed of bacteria  $V_b$  and the marker's velocity  $V_m$ ; see Fig. 2. This relationship was used later to reconstruct the swimming speed of bacteria from the marker's velocity in a thick film and at low magnification. We observed that when the velocity of the markers  $V_m$  approaches  $\approx 7 \mu\text{m/s}$ , the swimming speed of bacteria  $V_b$  approaches zero. The residual movement of the tracer particles is caused mainly by the "tracking" noise, e.g., tracers sink, go out of focus.

To prepare a medium with a known concentration of bacteria, we take a suspension of bacteria in a stationary phase of growing and split it into several 1.5 mL plastic tubes of known weight. The total weight of the tubes with the suspension was then measured. After centrifugation, the liquid from the tubes was removed and the weight of bacteria in each of the tubes was estimated to within an accuracy of 0.5 mg. Since the bacterial body is approximately a spherocylinder with aspect ratio  $\approx 7$  and the volume fraction of randomly dense packed spherocylinders of the same aspect ratio is  $\approx 0.5$  (see [17]), we can estimate the net weight of bacteria as half of the measured weight after centrifugation. The number of bacteria in each tube was found by using the fact that the mean bacterial weight is  $2.5 \times 10^{-12}$  g. Here we neglect fluctuations of bacterium size, and correspondingly, the variations of bacterium aspect ratio which can slightly increase the filling fraction. We then added liquid to each tube until it reached the desired concentration.

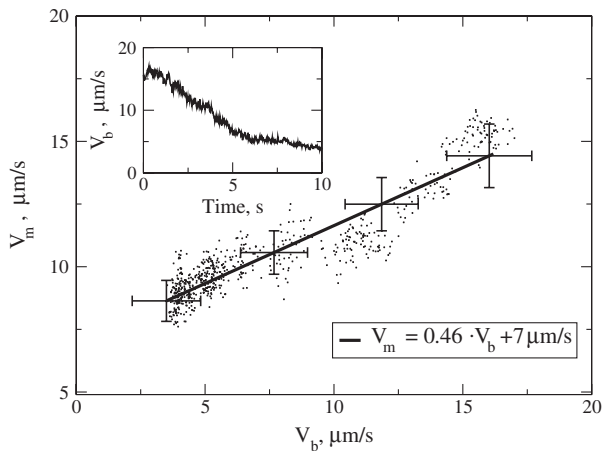


FIG. 2. Velocity of  $0.53 \mu\text{m}$  fluorescent markers vs swimming speed  $V_b$ . Dots depict experimental data; solid line is the fit  $V_m = 0.46V_b + 7$ . Inset: Swimming speed  $V_b$  vs time in the course of filling of the experimental chamber with nitrogen. Only part of the velocity decay is shown.

*Decay of a vortex.*—To initialize a vortex flow in a film, we used a custom-made micromanipulator built from the optical actuator taken from a commercial DVD-ROM. Two pairs of magnetic biasing coils control the horizontal and vertical position of the lens holder. The lens was replaced with a microprobe ( $0.5 \text{ mm}$  wire) (Fig. 1) to produce a vortex through short ( $0.5 \text{ mm}$ ) and fast ( $0.1 \text{ s}$ ) horizontal movement of the probe. Fluorescent  $2.54 \mu\text{m}$  tracer particles (Spherotech) were added to the suspension in order to visualize the flow.

We infer the viscosity from the time dependence of the tracer particles velocity during the decay of the probe-induced vortex. We assume that the liquid is incompressible and the flow is purely two-dimensional. The decay of the vortex of a characteristic size  $L$  occurs due to friction between the liquid and the container wall. If we neglect the spatial variations of the viscosity  $\nu$ , then in small Reynolds number limit the velocity  $\mathbf{V}$  of liquid satisfies the Navier-Stokes equation:  $\partial_t \mathbf{V} = -\nabla p + \nu \nabla^2 \mathbf{V}$ . Assuming rotation symmetry of the flow, the tangential component of velocity decays in time approximately as

$$V(t) \approx V_0 \exp\left(-\frac{a_0}{L^2} \int_0^t \nu(\tau) d\tau\right), \quad (1)$$

where  $V_0$  is the initial characteristic velocity,  $\nu$  is the shear viscosity (which can be a function of time  $t$ —e.g., through the dependence on the strain rate  $\dot{\gamma}(t)$ ), and  $a_0$  is a constant which depends on geometry of the cell. For a circular cell,  $a_0 = 4r_1 \approx 16$  where  $r_1 = 3.84$  is the first zero of the Bessel function  $J_1$ . For simplicity, we assume that the viscosity  $\nu$  is practically constant for small  $\dot{\gamma}$  and begins to depend on the strain rate only above a certain critical value  $\dot{\gamma}_c \approx V_b/l$ , where  $V_b$  and  $l$  are the typical swimming speed and size of bacterium, respectively [14]. To satisfy this assumption, we exclude the initial rapid stage of relaxation which typically last  $0.2$ – $1 \text{ s}$ . During this stage, the characteristic velocity of fluorescent tracers drops abruptly from  $5 \text{ mm/s}$  to  $200$ – $500 \mu\text{m/s}$ . During the following slower stage, the velocity decreases from  $200$ – $500 \mu\text{m/s}$  during  $1$ – $3 \text{ s}$  to a value defined by a chaotic motion of fluorescent tracers. For this stage the viscosity extracted from Eq. (1) is practically constant (see Fig. 3, inset). Thus, we substitute the simpler equation  $V(t) = V_0 \exp(-a_0 \nu t / L^2)$  for (1), yielding

$$\nu = -\frac{L^2}{a_0} \frac{d[\ln(V_a(t))]}{dt}, \quad (2)$$

where  $V_a(t)$  is the average flow velocity in the field of view of the microscope. The combination  $L^2/a_0$  can be found from an experiment where the viscosity is known (liquid without bacteria). We measured the viscosity for 6 different concentrations of bacteria; see Fig. 3. At very high concentrations the increase of viscosity occurs due to reduction of the bacterial motility [4]. In addition, in passive suspensions, the viscosity increases with volume fraction of particles.

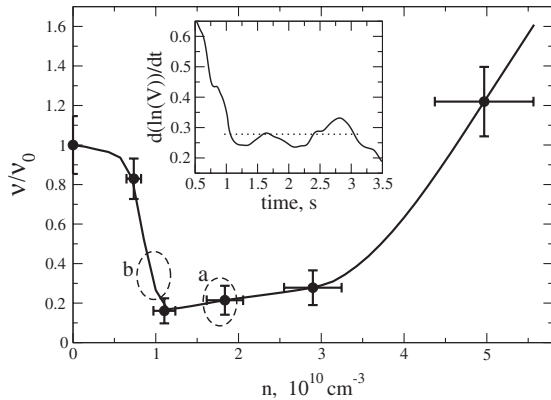


FIG. 3. Viscosity for 6 different concentrations of bacteria.  $\nu_0$  is the viscosity of the liquid without bacteria. Inset: instant viscosity vs time during decay of the vortex for density  $n = 2.9 \times 10^{10}$ . The dashed line is the average value of the viscosity during the slow phase of decay. See movies 1 and 2 in [19].

*Rotation of a magnetic particle.*—While the vortex decay technique offers a simple and intuitive way to estimate the viscosity, it is indirect and based on a number of assumptions about the flow structure, strain rate dependence, etc. To probe the viscosity directly, we used a technique based on measuring the viscous drag exerted on a rotating magnetic particle in a rotating magnetic field (see Fig. 4). We connected orthogonal pairs of magnetic coils through current amplifiers to synchronized function generators in order to create a magnetic field with a constant amplitude of 0–10 Gs rotating horizontally in the plane of the liquid film. A magnetized 100  $\mu\text{m}$  Nickel particle was placed in the center of the liquid film and was held in place by gravity (through the gravitational depression of the film). First, we determined the direction of the particle’s internal magnetic moment by applying a relatively strong constant magnetic field (10 Gs) of known direction, forcing the particle to align its magnetic moment with the direction of the applied field. Then, using custom-

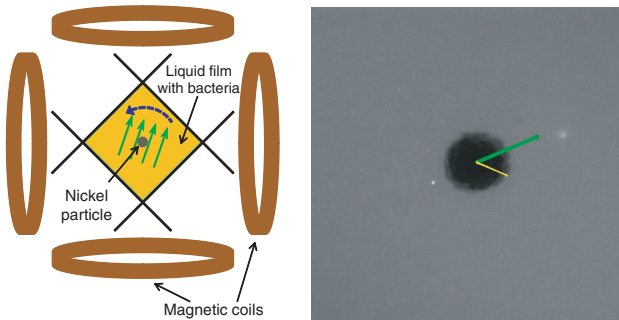


FIG. 4 (color online). Left: a thin liquid film containing a bacterial suspension and submersed Ni particle spanning between four movable fibers. Two pairs of magnetic coils create a rotating magnetic field (four green arrows). Right: Field of view of the microscope. The particle’s magnetic moment is shown by a short yellow arrow and the external magnetic field by a long green arrow. See movie 3 in [19].

made MATLAB software, we compared the image for an arbitrary position and orientation of the particle with the reference image and extracted the direction of the magnetic moment of our particle  $\alpha$ . This technique has much better precision than the corresponding integration of angular velocity of rotation. Second, we applied a rotating magnetic field  $H$  with an amplitude of 3 Gs and a rotational frequency of  $\Omega = 0.5$  Hz.

The viscosity  $\nu$  can be extracted from the balance of rotational viscous drag  $T_v \propto \nu \partial_t \alpha$  with the magnetic torque  $T_m \propto \mu_0 H \sin \phi$ , where  $\phi$  is the angle between the magnetic moment and the external field and  $\mu_0$  is the particle’s magnetic moment. In the case of synchronous rotation of the particle and field,  $\partial_t \alpha = \Omega$ , the viscosity can be extracted from the angle  $\phi$ , since  $\nu \sim (\sin \phi) / \Omega$ . We measured the orientation of the particle’s internal magnetic moment in each recorded frame while filling the chamber with  $N_2$ . Because of imperfection in the particle’s shape and a noncircular depression of the film by the particle, the angle  $\phi$  fluctuates slightly near its mean value (constant stray magnetic fields are excluded by precise calibration of our magnetic system). However, due to the change in the viscosity, the mean value of  $\phi$ , and correspondingly, magnetic torque  $T_m$  increases with time (Fig. 5) as the  $N_2/O_2$  ratio increases (hence the bacterial motility decreases). The particle stops rotating when the motility of the bacteria drops below some critical value: the viscosity of the suspension becomes so high that the torque required for rotation of the particle at constant rate  $\Omega$  is larger than the maximum magnetic torque.

In the course of filling the chamber with  $N_2$ , the torque averaged over the period of rotation increased from 0.15 to 1 (measured in units of maximal possible torque) and then

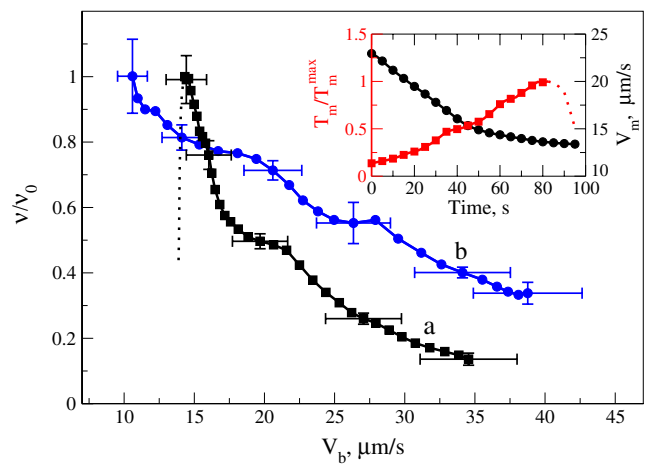


FIG. 5 (color online). Viscosity vs speed of the bacteria for two concentrations: (a)  $n \approx 1.8 \times 10^{10} \text{ cm}^{-3}$  (■) and (b)  $n \approx 10^{10} \text{ cm}^{-3}$  (●). Corresponding concentrations are indicated in Fig. 3 [areas (a) and (b)].  $\nu_0$  is the viscosity of the solution of immobilized bacteria. Inset: Magnetic torque  $T_m$  (■) calculated as  $\sin(\phi)$  and typical velocity of tracers  $V_m = 2\langle |V_r| \rangle$  (●) vs time. The dashed line shows the nonphysical values of  $T_m$  and  $\nu$  calculated for a magnetic particle that is stuck.

dropped due to termination of the rotation. Since the torque is proportional to the viscosity  $\nu$ , we obtained that the viscosity of the suspension at maximum swimming speed (which occurs when the chamber filled with air) was roughly 6–7 times lower than the viscosity of the same suspension of immobilized bacteria; see Fig. 5. Compared to our vortex decay experiment, we observed a similar trend: the viscosity of a bacterial suspension at the same concentration, in the presence of sufficient amount of oxygen, is one seventh the viscosity of the liquid without bacteria. However, since the suspension of immobilized bacteria has a slightly higher viscosity than the fluid, the relative viscosity reduction was even higher in the magnetic torque experiment.

In order to estimate simultaneously the typical swimming velocity of bacteria, we monitored the motion of fluorescent markers using a particle tracking technique. We used a highly dilute suspension of  $0.53 \mu\text{m}$  particles to track the motion of the bacteria. These particles are much smaller than those used in the vortex decay measurements, so some of them stick to the bacteria, making them perfect tracers for measuring the speed of bacteria. To exclude the effect of circular flow motion, we took into account only the absolute value of the radial component  $|V_r|$  of the velocity and estimated the magnitude of 3D velocity as  $2|V_r|$  (since we averaged only one component of 3D random motion). Because of nonspherical shape of the nickel particle, the radial motion of fluorescent markers in its proximity is affected by the rotation of particle. We averaged velocity of the markers only at distances greater than  $200 \mu\text{m}$  from the nickel particle. At low magnification (5X), we are able to track a sufficient amount of markers displaced by bacteria or advected by the flow produced mainly by bacteria, thus eliminating the influence of rotating particle imperfection on the velocity of markers. As one sees from Fig. 5 (inset), the velocity of the markers  $V_m$  decreases from  $23 \mu\text{m/s}$  to  $13 \mu\text{m/s}$  during the first 90 sec and then asymptotically approaches  $10\text{--}12 \mu\text{m/s}$  when the chamber is fully filled with nitrogen and the motility stops. Using the relation between  $V_m$  and  $V_b$ , see Fig. 2, we reconstruct the magnitude of the bacteria's swimming speed. We measured the viscosity for two different concentrations: (a)  $n \approx 1.8 \times 10^{10} \text{ cm}^{-3}$  and (b)  $n \approx 10^{10} \text{ cm}^{-3}$ . As we see from Fig. 5, when the bacteria are motile, the viscosity of the more concentrated suspension (a) is smaller than that of the less concentrated one (b), in agreement with the results shown in Fig. 3. The situation reverses when the bacteria are "paralyzed" by the lack of oxygen: viscosity of the more concentrated suspension (a) is larger than that of the suspension (b).

In additional experiments, we confirmed the reversibility of the process. After the chamber was fully filled with nitrogen, we increased the concentration of oxygen, which resulted in an increase in the motility of the bacteria and a

decrease of the viscosity almost to the initial value. The difference between the initial and final levels of the viscosity likely stemmed from a change in the concentration of chemicals in the fluid due to the metabolism of the bacteria and from the evaporation of water from the film.

In conclusion, from two complementary experiments, we observed that the viscosity of a bacterial suspension strongly depends on the concentration and swimming speed of the bacteria. The effective viscosity of a suspension of bacteria at concentrations  $\approx 1\text{--}3 \times 10^{10} \text{ cm}^{-3}$  is 7 times lower than the viscosity of the liquid without bacteria. While our experiments were conducted for moderately dense suspensions of bacteria, the results are in qualitative agreement with theoretical predictions for dilute suspensions of swimmers in two dimensions [14] and in three dimensions [18]. The mechanism for the viscosity reduction is transformation by bacteria of chemical energy of the nutrient into kinetic energy of fluid motion.

This work was supported by the US DOE, Office of Basic Energy Sciences, contract DEAC02-06CH11357.

- 
- [1] X.-L. Wu and A. Libchaber, Phys. Rev. Lett. **84**, 3017 (2000).
  - [2] C. Dombrowski *et al.*, Phys. Rev. Lett. **93**, 098103 (2004); I. Tuval *et al.*, Proc. Natl. Acad. Sci. U.S.A. **102**, 2277 (2005).
  - [3] D. Saintillan and M.J. Shelley, Phys. Rev. Lett. **99**, 058102 (2007); Phys. Rev. Lett. **100**, 178103 (2008).
  - [4] A. Sokolov, I. S. Aranson, J.O. Kessler, and R.E. Goldstein, Phys. Rev. Lett. **98**, 158102 (2007).
  - [5] A. P. Berke *et al.*, Phys. Rev. Lett. **101**, 038102 (2008).
  - [6] J.P. Hernandez-Ortiz, C.G. Stoltz, and M.D. Graham, Phys. Rev. Lett. **95**, 204501 (2005).
  - [7] K. Drescher *et al.*, Phys. Rev. Lett. **102**, 168101 (2009).
  - [8] I. H. Riedel, K. Kruse, and J. Howard, Science **309**, 300 (2005).
  - [9] I.D. Couzin and J. Krause, Adv. Study Behav. **32**, 1 (2003).
  - [10] K. Kruse *et al.*, Phys. Rev. Lett. **92**, 078101 (2004).
  - [11] R. A. Simha and S. Ramaswamy, Phys. Rev. Lett. **89**, 058101 (2002).
  - [12] I. S. Aranson, A. Sokolov, J.O. Kessler, and R.E. Goldstein, Phys. Rev. E **75**, 040901(R) (2007).
  - [13] Y. Hatwalne *et al.*, Phys. Rev. Lett. **92**, 118101 (2004).
  - [14] B. M. Haines *et al.*, Phys. Biol. **5**, 046003 (2008).
  - [15] D. T. N. Chen *et al.*, Phys. Rev. Lett. **99**, 148302 (2007).
  - [16] C. Douarche *et al.*, Phys. Rev. Lett. **102**, 198101 (2009).
  - [17] S. R. Williams and A. P. Philipse, Phys. Rev. E **67**, 051301 (2003).
  - [18] B. M. Haines, A. Sokolov, I. S. Aranson, L. Berlyand, and D. A. Karpeev (to be published).
  - [19] See EPAPS Document No. E-PRLTAO-103-058942 for auxiliary files containing experimental movies. For more information on EPAPS, see <http://www.aip.org/pubservs/epaps.html>.